

Synthesis, characterization, photochromism and theoretical interpretation of bis-(triphenylphosphine)-Cu(I)- and Ag(I)-(1-alkyl-2-(arylo)imidazole) complexes

Bharati Chowdhury^a, Kaushik Naskar^a, Debashis Mallick^{*b}, Chandana Sen^c,
Kamal Krishna Sarkar^d and Chittaranjan Sinha^{*a}

^aDepartment of Chemistry, Jadavpur University, Kolkata-700 032, India

E-mail: crsjuchem@gmail.com

^bDepartment of Chemistry, Mrinalini Datta Mahavidyapith, Birati, Kolkata-700 051, India

E-mail: dmchemmdm51@gmail.com

^cDepartment of Chemistry, Sripat Singh College, Murshidabad-742 123, West Bengal, India

^dDepartment of Chemistry, Mahadevananda Mahavidyalaya, S. N. Banerjee Rd., Monirampore, Kolkata-700 120, India

Manuscript received 09 January 2018, revised 07 March 2018, accepted 08 March 2018

Abstract: [Cu(PPh₃)₂(RaaiR')]ClO₄ and [Ag(PPh₃)₂(RaaiR')]NO₃ (RaaiR', 1-alkyl-2-(arylo)imidazole) complexes are spectroscopically characterised and in one case, [Cu(PPh₃)₂(HaaiMe)]ClO₄ (3a), the structure is confirmed by single crystal X-ray diffraction measurement. UV light irradiation to the solution of the complexes in DMF (free ligand in MeOH) show *trans*-to-*cis* isomerisation about -N=N-C₆H₄-R. The reverse transformation, *cis*-to-*trans*, is carried out under thermal condition. Quantum yields ($\phi_{t \rightarrow c}$) of *trans*-to-*cis* isomerisation of free ligand is higher than their complex phase. The activation energy (E_a) of *cis*-to-*trans* isomerisation is calculated by controlled temperature experiment and is found that E_a (ligands) > E_a (complexes). The Density Functional Theory has been used to calculate electronic structure of the optimized geometry and hence the interpretation of the spectral and photochromic properties.

Keywords: Aryloimidazole, PPh₃, copper(I) and silver(I) complexes, single crystal X-ray, photochromism, DFT computation.

Introduction

Azo dyes, an essential class of molecules in coloring industries, have been used as photostable and weather stable pigments¹. Recently, some metal complexes of dyes have found applications in the realm of high-technology area such as photoelectronic devices, optical recording media², light emitting diodes³, field effect transistors⁴, photovoltaic cells⁵ etc. 1-Alkyl-2-(arylo)imidazole (RaaiR'), a heterocyclic-azo derivative, has been used in the focus of coordination chemistry and are useful for optical materials⁶. These molecules undergo reversible photo-induced transformation between *cis* and *trans* isomers about -N=N- whose absorption spectra differ

significantly⁷ and is defined as photochromism. RaaiR' may act as N(imidazolyl), monodentate and/or N(imidazolyl), N(azo) bidentate chelating ligand^{8,9}. The photochromic behavior of RaaiR'⁶ and some of the complexes like Zn(II)¹⁰, Cd(II)¹¹, Hg(II)¹², Pb(II)¹³ and Pd(II)¹⁴-azoimidazoles has motivated us to examine the photochromic property of Cu(I) and Ag(I) complexes.

The chemistry of copper(I) and silver(I) with azoimine (-N=N-C=N-) functional group has brought a considerable attention¹⁵ because of their interesting electronic, optical, structural, biological, redox and catalytic properties¹⁶. *p*-Acidic azoimine (-N=N-C=N-) group stabilizes low valent metal redox state.

The presence of other π -acidic molecules like, PPh_3 , CO, NO cooperate the azoimine function to stabilize low redox state like Cr(0), Mo(0), W(0), Ru(0)¹⁷, Cu(I)¹⁵. Herein we report hitherto unknown ternary Cu(I) and Ag(I)-complexes of RaaiR' and PPh_3 . This article describes the structures, spectral properties and photochromism of the complexes. DFT computation has been attempted to correlate with the experimental and theoretical structure parameter and electronic properties of the representative complexes.

Results and discussion

Synthesis and formulation of compounds:

1-Alkyl-2-(arylazo)imidazole [RaaiR' , where R = H (**a**), Me (**b**); $\text{R}' = \text{Me}$ (**1**) and Et (**2**)], react with $\text{Cu}(\text{MeCN})_4\text{ClO}_4$, Ph_3P in 1:1:2 mole ratio in dry MeOH solution which has isolated $[\text{Cu}(\text{PPh}_3)_2(\text{RaaiR}')]\text{ClO}_4$. Under identical condition reaction between RaaiR' , PPh_3 and AgNO_3 , in mixed solvent of acetonitrile and MeOH has isolated $[\text{Ag}(\text{PPh}_3)_2(\text{RaaiR}')]\text{NO}_3$. Microanalytical data support the composition of the complexes. In infrared spectra of RaaiR' the $\nu(\text{N}=\text{N})$ and $\nu(\text{C}=\text{N})$ appear at 1400–1410 and 1620–1625 cm^{-1} and in the complexes these bands are shifted to lower frequency, 1370–1385 and

1530–1560 cm^{-1} respectively which are in support of coordination of azo-N and imine-N to M(I) (Table 1). The molar conductivity of the complexes, 70–90 $\Omega^{-1} \text{mol}^{-1} \text{cm}^2$ in DMF, supports the 1:1 conductivity of the complexes.

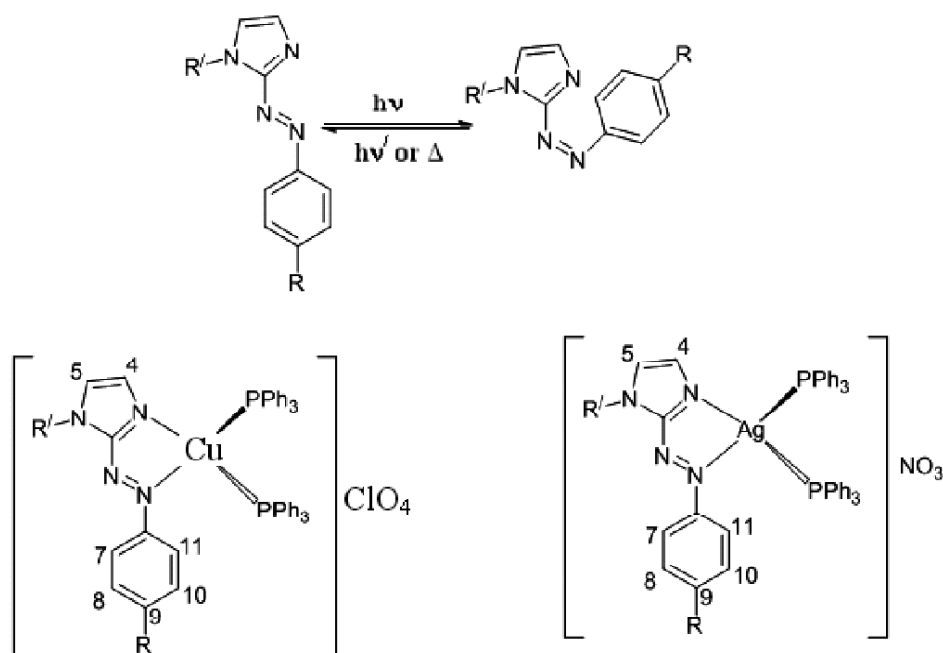
The solution electronic spectra of RaaiR' in methanol show a transition at 340–380 nm with a molar absorption coefficient in the order of $10^3 \text{ M}^{-1} \text{ cm}^2$ and a tail extending into 550 nm with a weak band at 470–490 nm. The intense absorption band corresponds to π - π^* transitions, while the tail corresponds to n - π^* transition¹⁵.

The ¹H NMR spectra of complexes in CDCl_3 reveal that the signals in the complexes are shifted to downfield side relative to free ligand values. This supports the coordination of ligand to M(I). Important feature of the spectra is the shifting of imidazole protons 4-H and 5-H to lower δ -values, in general, relative to aryl protons (7-H–11-H). Imidazole protons suffer downfield shifting by 0.3–0.4 ppm compared to the free ligand position (Table 1). This supports the strong preference of binding of imidazole-N to metal. Aryl signals shift to the lower field side on Me-substitution to the aryl ring. This is due to electron donating effect of the Me- group.

Table 1. ¹H NMR spectral data of the complexes in CDCl_3 at room temperature

Compd. ^a	δ (ppm)								
	4-H ^s	5-H ^s	7,11-H ^d	8,10-H ^d	9-Me	1-Me	1-CH ₂ ^q	(1-CH ₂)-CH ₃ ^t	PPh_3 ^m
3a	7.52	7.25	7.98 (8.0)	7.31	–	4.23	–	–	7.46–7.75
3b	7.49	7.20	7.89 (8.1)	7.28 (7.9)	2.42	4.21	–	–	7.45–7.70
4a	7.50	7.21	7.96 (7.9)	7.30	–	–	4.53 (7.5)	1.57 (8.2)	7.45–7.74
4b	7.48	7.19	7.86 (8.1)	7.31 (8.1)	2.44	–	4.52 (7.5)	1.59 (8.1)	7.41–7.73
5a	7.74	7.30	8.10 (8.2)	7.32	–	4.28	–	–	7.44–7.72
5b	7.71	7.26	8.06 (7.9)	7.27 (8.0)	2.43	4.25	–	–	7.47–7.71
6a	7.70	7.27	8.07 (8.0)	7.26	–	–	4.60 (7.5)	1.59 (8.1)	7.46–7.71
6b	7.68	7.27	7.80 (8.1)	7.29 (8.1)	2.43	–	4.59 (7.6)	1.62 (8.2)	7.44–7.70

^a¹H NMR spectral data of HaaiMe (**1a**), MeaaiMe (**1b**), HaaiEt (**2a**), MeaaiEt (**2b**) are obtained for comparison from Reference 15(a); ^sSinglet; ^dDoublet; ^tTriplet; ^qQuartet; ^mMultiplet.



Scheme 1. Photo-isomerization of 1-alkyl-2-(arylamino)imidazole [(R = H (**a**), Me (**b**); R' = Me (**1**) and Et (**2**), [Cu(PPh₃)₂-(RaaiR')](ClO₄) [(R = H (**a**), Me (**b**); R' = Me (**3**) and Et (**4**)] and [Ag(PPh₃)₂(RaaiR')](NO₃) [(R = H (**a**), Me (**b**); R' = Me (**5**) and Et (**6**)).

*Molecular structure of [Cu(PPh₃)₂(HaaiMe)]ClO₄ (**3a**):*

The crystals of [Cu(PPh₃)₂(HaaiMe)]ClO₄ (**3a**) are obtained by slow evaporation of the synthetic reaction mixture in MeOH at ambient condition for a week in dark. The molecular structure is shown in Fig. 1. The bond parameters are listed in Table 2. Each discrete molecular unit consists of tetrahedral coordination CuN₂P₂ fragment. HaaiMe acts as bidentate N(azo), N(imidazolyl) chelator. The atomic arrangements Cu(1), N(4), N(3), C(39), N(1) constitute the chelate plane with a maximum deviation

Table 2. Selected bond lengths (Å) and angles (°) of [Cu(HaaiMe)(PPh₃)₂]ClO₄ (**3a**)

Bond lengths (Å)		Bond angles (°)	
Cu(1)-N(1)	2.071(4)	N(1)-Cu(1)-N(4)	77.37(14)
Cu(1)-N(4)	2.116(4)	N(1)-Cu(1)-P(2)	112.51(11)
Cu(1)-P(2)	2.2574(12)	N(4)-Cu(1)-P(2)	109.37(10)
Cu(1)-P(1)	2.2688(12)	N(1)-Cu(1)-P(1)	113.77(10)
N(3)-N(4)	1.273(5)	N(4)-Cu(1)-P(1)	110.76(11)
N(1)-C(39)	1.328(6)	P(2)-Cu(1)-P(1)	123.52(5)
N(3)-C(39)	1.379(6)	C(46)-N(4)-Cu(1)	127.7(3)
N(4)-C(46)	1.423(6)	N(1)-C(39)-N(2)	112.4(4)
N(2)-C(39)	1.350(6)	N(3)-N(4)-Cu(1)	116.9(3)

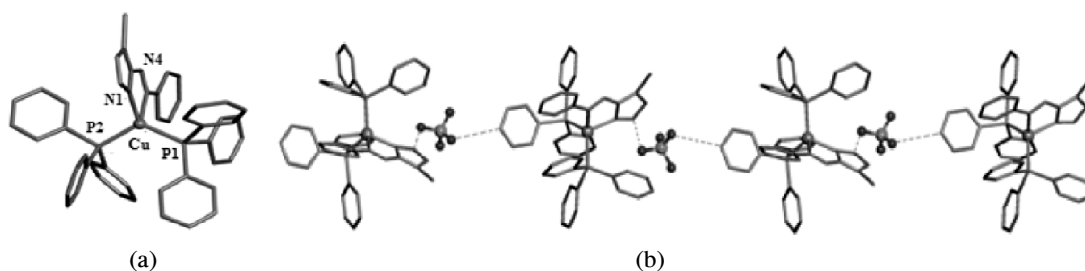


Fig. 1. (a) Molecular structure of **3a** and (b) hydrogen bonded 1D chain.

$<0.04 \text{ \AA}$. The pendant phenyl ring makes a small dihedral 4.7° with chelated azoimidazole ring. The small chelate angle $\angle N(1)\text{-Cu}(1)\text{-N}(4)$, $(77.37(14)^\circ)$ may be one of the reasons for geometrical distortion.

The Cu(1)-N(imidazolyl) (Cu(1)-N(1), $2.071(4) \text{ \AA}$) is shorter than Cu(1)-N(azo) (Cu(1)-N(4), $2.116(4) \text{ \AA}$), which reflects stronger interaction between Cu(I) and N(imidazolyl). Although Cu(1)-N(azo) bond length is very long but it is less than the sum of van der Waals radii of Cu(I) (1.40 \AA) and N(sp^2) (1.53 \AA). This implies significant bonding interaction between these components. The stronger coordination of imidazole-N to Cu(I) compared to azo-N has significant biochemical and photochemical implication and explains photostability of Ag(I)¹⁵. Because of long Cu(I)-N(azo) distance, the molecule becomes useful for photo-activation via cleavage of this bond followed by rotation to induce photoisomerisation (*vide infra*). The N=N distance is $1.273(5) \text{ \AA}$ and is comparable to previously reported result ($1.262(6) \text{ \AA}$)¹⁵.

Photochromism:

The chelated ligand, RaaiR' in the complexes undergo photo-induced isomerisation and the quantum yields of the *trans*-to-*cis* photoisomerisation are noted in Table 3. The intense peak at λ_{max} in DMF solution ($\sim 360 \text{ nm}$) of the complexes decreases, which

is accompanied by a slight increase at the tail portion of the spectrum around 485 nm until a stationary state (PS-I) is reached (Fig. 2). Upon UV light irradiation *trans* structure of RaaiR' changes to *cis* structure about the azo (-N=N-) function and the *cis* molar ratio reaches to $>95\%$ (Scheme 1). The complexes are resistant to photo degradation upon repeated irradiation at least up to 15 cycles in each case. In the complexes the $\phi_{t \rightarrow c}$ values are significantly less than that of free ligand data.

Table 3. Results of photochromism, rate of conversion and quantum yields upon UV light irradiation

Compounds	λ_{π, π^*} (nm)	Isobestic point (nm)	Rate of t→c conversion $\times 10^8 \text{ (s}^{-1}\text{)}$	$\phi_{t \rightarrow c}$ conversion $\times 10^8$
HaaiMe (1a) ^a	363	333,431	5.06	0.25
HaaiEt (2a) ^a	364	334,433	4.83	0.24
MeaaiMe (1b) ^a	365	331,443	3.70	0.218
MeaaiEt (2b) ^a	365	328,444	4.59	0.206
3a	366	333,448	3.35	0.10
3b	362	327,437	1.29	0.06
4a	365	333,448	0.78	0.04
4b	367	332,447	0.82	0.05
5a	378	325,444	0.88	0.049
5b	380	333,447	1.47	0.058
6a	361	324,424	0.98	0.05
6b	363	327,436	0.44	0.04

^aData are collected from Ref. 6.

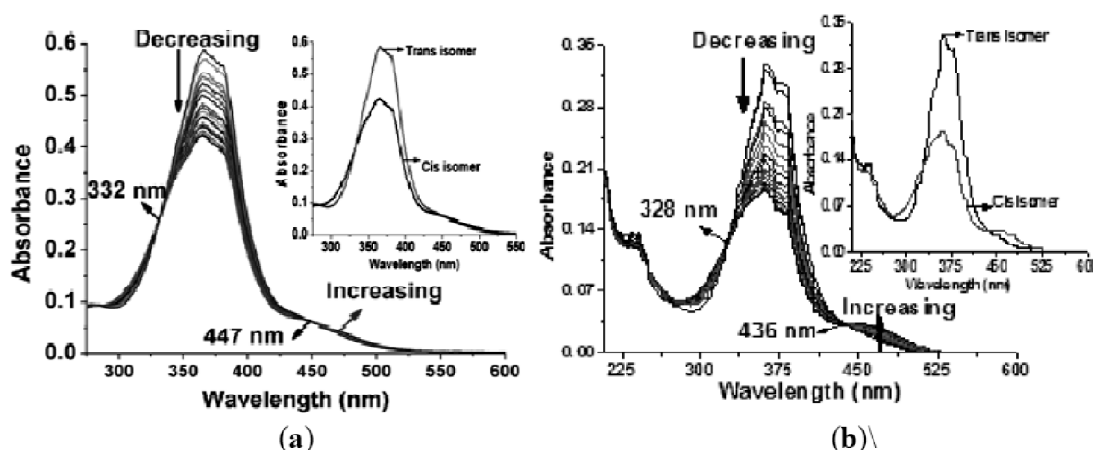


Fig. 2. Spectral changes of *trans*-to-*cis* isomerisation of coordinated MeaaiMe of (a) $[\text{Cu}(\text{PPh}_3)_2(\text{MeaaiMe})]\text{ClO}_4$ (**3b**) and (b) $[\text{Ag}(\text{PPh}_3)_2(\text{MeaaiMe})]\text{NO}_3$ (**5b**) in MeOH upon repeated irradiation at 366 nm at 3 min interval at 25°C . Inset figure shows spectra of *cis* and *trans* isomer of the complex.

The *cis*-to-*trans* isomerisation of RaaiR' in the complexes **3-6** are examined at varied temperatures, 306–321 K (Table 4, Fig. 3) followed by spectral measurements. The Eyring plots in the temperature range 306–321 K gave a linear plot from which the activation parameters ΔS^* and ΔH^* are calculated (Table 4, Fig. 4). In the complexes, the E_a s are severely decreased which means faster *cis*-to-*trans* thermal isomerisation of RaaiR' in the complexes. The entropy of activation (ΔS^*) are high negative in the complexes than that of free ligand. This is also in support of increase in rotor mass of the complexes.

DFT Computation and Frontier molecular orbitals:

The structures of $[\text{Cu}(\text{PPh}_3)_2(\text{MeaaiMe})]^+$ (**3b**) and $[\text{Ag}(\text{PPh}_3)_2(\text{MeaaiMe})]^+$ (**5b**) are optimized by DFT computation. The MOs like HOMO, HOMO-1 and HOMO-2 of **3b** are closely spaced (E_{HOMO} , -8.24 eV; $E_{\text{HOMO-1}}$, -8.45 eV; $E_{\text{HOMO-2}}$, -8.62 eV) where as in the case of unoccupied molecular orbitals such as LUMO+1 and LUMO+2 are intimately associated except LUMO (E_{LUMO} , -5.53 eV; $E_{\text{LUMO+1}}$, -3.03 eV; $E_{\text{LUMO+2}}$, -3.00 eV). In **5b** occupied molecular orbitals are lower in energy than that of **3b** (E_{HOMO} , -8.31 eV; $E_{\text{HOMO-1}}$, -8.59 eV;

Table 4. Rate and activation parameters for *cis* (c) \rightarrow *trans* (t) thermal isomerisation

Compounds	Temp. (K)	Rate of thermal c \rightarrow t conversion $\times 10^4$ (s $^{-1}$)	E_a (kJ mol $^{-1}$)	ΔH^* (kJ mol $^{-1}$)	ΔS^* (J mol $^{-1}$ K $^{-1}$)	ΔG^* (kJ mol $^{-1}$)
HaaiMe (1a) ^a	306	0.22	79.0	77.05	-77.1	100.00
	311	0.40				
	316	0.88				
	321	2.75				
MeaaiMe (1b) ^a	306	0.73	87.57	85.03	-38.84	96.60
	311	1.20				
	316	2.60				
	321	3.70				
HaaiEt (2a) ^a	306	0.33	86.87	84.33	-47.83	98.58
	311	0.50				
	316	0.97				
	321	1.80				
MeaaiEt (2b) ^a	306	0.64	87.63	87.08	-40.20	97.06
	311	0.98				
	316	1.87				
	321	3.40				
3a	306	3.132	55.63	53.02	-139.03	42.59
	311	4.301				
	316	6.281				
	321	8.592				
3b	306	3.821	59.41	56.802	-124.9	38.28
	311	5.708				
	316	7.735				
	321	11.6				
4a	306	5.458	61.26	58.65	-116.03	35.56
	311	8.002				
	316	10.7				
	321	15.3				

Table-4 (contd.)

4b	306	5.056	60.59	57.99	-99.51	30.51
	311	7.012				
	316	12.54				
	321	14.32				
5a	306	4.60	58.49	55.88	-126.62	40.70
	311	6.23				
	316	9.01				
	321	13.44				
5b	306	3.68	64.37	61.77	-108.8	33.35
	311	5.81				
	316	8.64				
	321	11.98				
6a	306	5.24	54.59	51.99	-137.67	42.18
	311	7.91				
	316	11.61				
	321	14.02				
6b	306	7.095	90.38	56.04	-74.74	22.92
	311	9.586				
	316	15.01				
	321	19.17				

^aData are collected from Ref. 6.

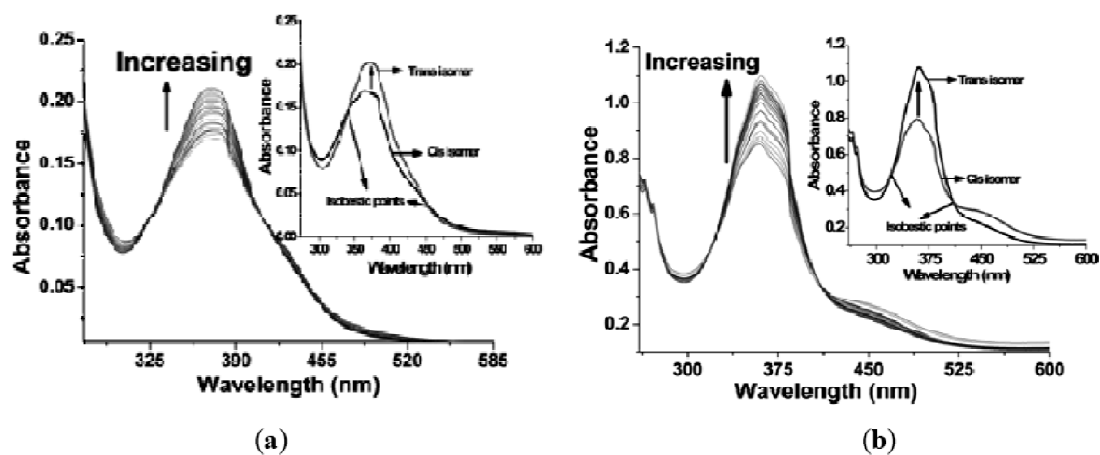


Fig. 3. Spectral changes of *cis*-to-*trans* isomerisation of (a) $[\text{Cu}(\text{PPh}_3)_2(\text{MeaaiMe})]\text{ClO}_4$ (**3b**) and (b) $[\text{Ag}(\text{PPh}_3)_2(\text{MeaaiMe})]\text{NO}_3$ (**5b**) in MeOH at 3 min interval at 306 K at thermal condition. Inset figure shows spectra of *cis* and *trans* isomer of the complex.

$E_{\text{HOMO}-2}$, -8.75 eV) and the UMOs also follow similar trend. Calculation shows that the occupied MOs of **3b** are mainly composed of metal and PPh_3 while unoccupied MOs are made of PPh_3 except LUMO where contribution of MeaaiMe is 95%. In **5b** occupied MOs are mainly contributed by MeaaiMe with

feeble contribution of PPh_3 in some functions; the UMOs are mainly contributed from PPh_3 along with Ag and MeaaiMe (LUMO-Ag 53%; MeaaiMe 5%, PPh_3 41% and LUMO + 1-Ag 3%; MeaaiMe 95%, PPh_3 2%). The energy correlation of the complexes is shown in Fig. 5.

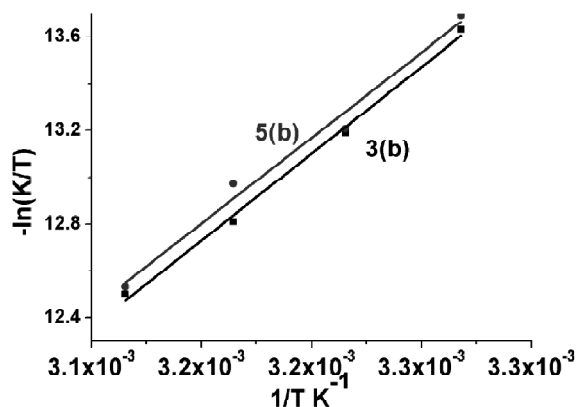


Fig. 4. The Eyring plots of rate constants of Z-to-E isomerisation of (a) $[\text{Cu}(\text{MeaiMe})(\text{PPh}_3)_2](\text{ClO}_4)$ (**3b**) and (b) $[\text{Ag}(\text{PPh}_3)_2(\text{MeaiMe})](\text{NO}_3)$ (**5b**) at 306–321 K.

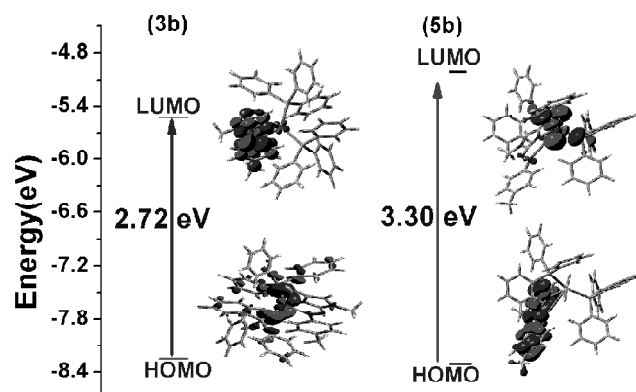


Fig. 5. Correlation energy diagram of $[\text{Cu}(\text{PPh}_3)_2(\text{MeaiMe})]\text{ClO}_4$ (**3b**) and $[\text{Ag}(\text{PPh}_3)_2(\text{MeaiMe})]\text{NO}_3$ (**5b**).

The electronic transitions in the complexes may be associated with intra-ligand charge transfer (XLCT)

and metal-ligand charge transfer or vice versa (MXCT/XMCT) (Table 4). Both the compounds, **3b** and **5b**, exhibit intense transitions at 350–380 nm along with an additional band at 400–415 nm is noticeable. The band at 330–380 nm is referred to $n/\pi(\text{PPh}_3) \rightarrow \pi^*(\text{N}=\text{N})$ in case of **3b** and $n/\pi(\text{PPh}_3) \rightarrow \text{Ag}$ i.e. the case of **5b** while the transitions 250–200 nm is assigned to $\text{M}(\text{I}) \rightarrow \pi^*(\text{PPh}_3)$.

Experimental

Materials: AgNO_3 , methyl iodide, ethyl iodide were obtained from Sigma-Aldrich. 1-Alkyl-2-(arylo)imidazoles were synthesized by reported procedure¹⁵. $[\text{Cu}(\text{CH}_3\text{CN})_4](\text{ClO}_4)$ was prepared in the laboratory using standard method. All other chemicals and solvents were reagent grade and used as received and the solvents were purified before use by standard procedure¹⁸.

Physical measurements:

Microanalytical data (C, H, N) were collected on Perkin-Elmer 2400 CHNS/O elemental analyzer. Spectroscopic data were obtained using the following instruments: UV-Vis spectra from a Perkin-Elmer Lambda 25 spectrophotometer; IR spectra (KBr disk, $4000\text{--}400\text{ cm}^{-1}$) from a Perkin-Elmer RX-1 FTIR spectrophotometer; photo excitation has been carried out using a Perkin-Elmer LS-55 spectrofluorimeter and ^1H NMR spectra were recorded from a Bruker (AC) 300 MHz FTNMR spectrometer.

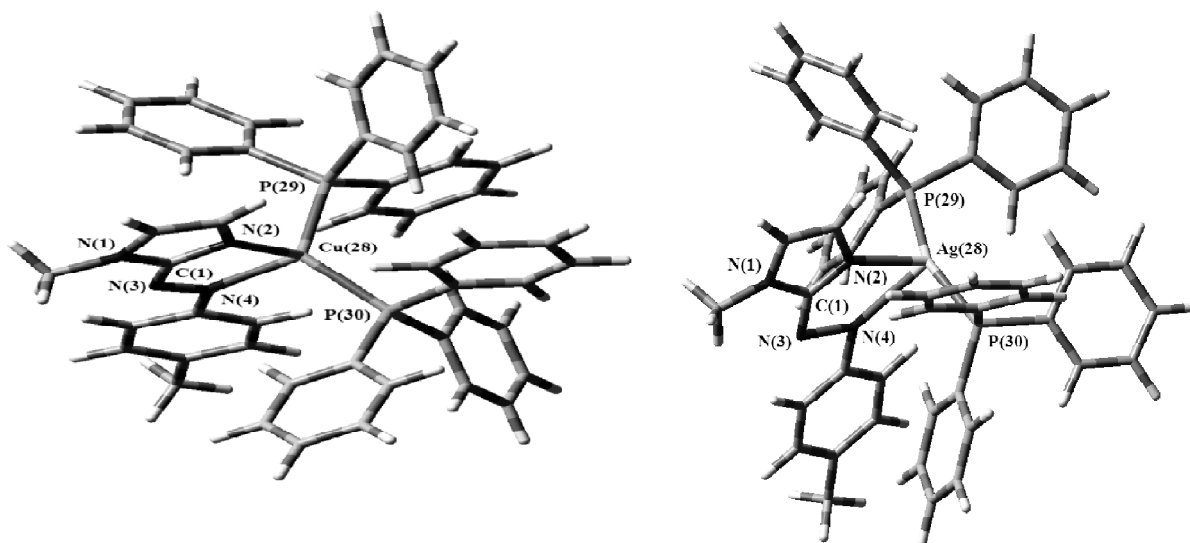
Synthesis of $[\text{Cu}(\text{PPh}_3)_2(\text{MeaiMe})]\text{ClO}_4$ (**3b**):

To acetonitrile solution (10 ml) of MeaiMe (13.34

Table 5. The spectral transitions calculated by TD-DFT computation of $[\text{Cu}(\text{PPh}_3)_2(\text{MeaiMe})]^+$ (**3b**) and $[\text{Ag}(\text{PPh}_3)_2(\text{MeaiMe})]^+$ (**5b**) in gaseous state

Excitation energy (eV)	Wavelength (nm)	<i>f</i>	Key transitions	Character
$[\text{Cu}(\text{PPh}_3)_2(\text{MeaiMe})]^+$ (3b)				
3.0723	403.55	0.1748	(49%) HOMO-13→LUMO	XLCT
3.4561	358.74	0.0358	(70%) HOMO-5→LUMO	XLCT
4.5168	274.49	0.2550	(78%) HOMO→LUMO+3	MXCT
$[\text{Ag}(\text{PPh}_3)_2(\text{MeaiMe})]^+$ (5b)				
3.2047	386.88	0.6046	(54%) HOMO-2→LUMO	XMCT
3.3511	369.98	0.0423	(67%) HOMO-4→LUMO	XMCT
4.0148	308.50	0.0573	(70%) HOMO-15→LUMO	XMCT

X- PPh_3 ; L-MeaiMe; XLCT: Intra-ligand charge transfer transition (PPh_3 to π^* of MeaiMe); MXCT: Cu/Ag to PPh_3 charge transfer transition.



[Cu(PPh₃)₂(MeaaiMe)]⁺ unit of **3b**
 Cu(28)-N(2), 2.10407; Cu(28)-N(4), 2.18735; N(3)-N(4),
 1.30740; Cu(28)-P(29), 2.41695; Cu(28)-P(30), 2.42663;
 ∠N(2)-Cu(28)-N(4), 77.98650.

[Ag(PPh₃)₂(MeaaiMe)]⁺ unit of **5b**
 Ag(28)-N(2), 2.62086; Ag(28)-N(4), 2.42435; N(3)-N(4),
 1.29334; Ag(28)-P(29), 2.48449; Ag(28)-P(30), 2.48736;
 ∠N(2)-Ag(28)-N(4), 82.94650.

Fig. 6. Optimized structures of [Cu(PPh₃)₂(MeaaiMe)]⁺ (**3b**) and [Ag(PPh₃)₂(MeaaiMe)]⁺ (**5b**) drawn by using DFT-B3LYP function along with important bond parameters.

mg, 0.07 mmol), [Cu(CH₃CN)₄](ClO₄) (22.89 mg, 0.07 mmol) in methanol (5 ml) was added followed by PPh₃ (36.70 mg, mmol) and magnetically stirred for 3 h. The solution was then filtered and the filtrate was slowly evaporated in dark. Black crystals were deposited on glass wall and then collected cautiously and washed with n-hexane. The yield was 58.06 mg (79%).

Other compounds were prepared following identical procedure. Yield varied from 70–80%.

Microanalytical data of the complexes are as follows: [Cu(Ph₃P)₂(HaaiMe)]ClO₄ (**3a**): Anal. Calcd. for C₄₆H₄₀N₄P₂O₄ClCu: C, 56.37; H, 4.11; N, 5.72. Found: C, 56.41; H, 4.09; N, 5.71; FT-IR (KBr disc, cm⁻¹): ν(N=N), 1419; ν(C=N), 1531 cm⁻¹; UV-Vis spectroscopic data in CHCl₃ (λ_{max}(nm) (10⁻³ ε (dm³ mol⁻¹ cm⁻¹)): 366 (28.0), 450 (2.84). [Cu(Ph₃P)₂(MeaaiMe)]ClO₄ (**3b**): Anal. Calcd. for C₄₇H₄₂N₄P₂O₄ClCu: C, 56.78; H, 4.26; N, 5.64. Found: C, 56.81; H, 4.23; N, 5.61; FT-IR (KBr disc, cm⁻¹): ν(N=N), 1422; ν(C=N), 1540 cm⁻¹;

UV-Vis spectroscopic data in CHCl₃ (λ_{max}(nm) (10⁻³ ε (dm³ mol⁻¹ cm⁻¹)): 366 (24.6), 449 (3.90). [Cu(Ph₃P)₂(HaaiEt)]ClO₄ (**4a**): Anal. Calcd. for C₄₇H₄₂N₄P₂O₄ClCu: C, 56.78; H, 4.26; N, 5.64. Found: C, 56.81; H, 4.23; N, 5.61; FT-IR (KBr disc, cm⁻¹): ν(N=N), 1418; ν(C=N), 1540 cm⁻¹; UV-Vis spectroscopic data in CHCl₃ (λ_{max}(nm) (10⁻³ ε (dm³ mol⁻¹ cm⁻¹)): 365 (15.8), 453 (3.10). [Cu(Ph₃P)₂(MeaaiEt)]ClO₄ (**4b**): Anal. Calcd. for C₄₈H₄₄N₄P₂O₄ClCu: C, 57.18; H, 4.40; N, 5.56. Found: C, 57.21; H, 4.39; N, 5.52; FT-IR (KBr disc, cm⁻¹): ν(N=N), 1425; ν(C=N), 1530 cm⁻¹; UV-Vis spectroscopic data in CHCl₃ (λ_{max}(nm) (10⁻³ ε (dm³ mol⁻¹ cm⁻¹)): 367 (21.8), 453 (4.40).

Synthesis of [Ag(PPh₃)₂(HaaiEt)]NO₃ (**6a**):

To acetonitrile solution (10 ml) of HaaiEt (13.40 mg, 0.07 mmol), AgNO₃ (11.90 mg, 0.07 mmol) in methanol (5 ml) was added followed by PPh₃ (36.68 mg, 0.14 mmol) in absence of light and magnetically stirred for 5 h. The solution was then filtered and the filtrate was slowly evaporated in dark. Orange crys-

tals were deposited on glass wall and then collected cautiously and washed with n-hexane. The yield was 51.06 mg (82%).

Other compounds were prepared following identical procedure. Yield varied from 75–83%.

Microanalytical data of the complexes are as follows: [Ag(Ph₃P)₂(HaaiMe)](NO₃) (**5a**): Anal. Calcd. for C₄₆H₄₀N₅O₃P₂Ag: C, 54.37; H, 4.07; N, 5.52. Found: C, 54.21; H, 4.16; N, 5.51; FT-IR (KBr disc, cm⁻¹): ν(N=N), 1435; ν(C=N), 1558 cm⁻¹; UV-Vis spectroscopic data in CHCl₃ (λ_{max}(nm) (10⁻³ ∈ (dm³ mol⁻¹ cm⁻¹)): 359 (32.3), 445 (2.34). [Ag(Ph₃P)₂(MeaaiMe)]NO₃ (**5b**): Anal. Calcd. for C₄₇H₄₂N₅O₃P₂Ag: C, 55.07; H, 4.62; N, 11.07. Found: C, 54.94; H, 4.55; N, 11.18; FT-IR (KBr disc, cm⁻¹): ν(N=N), 1436; ν(C=N), 1559 cm⁻¹; UV-Vis spectroscopic data in CHCl₃ (λ_{max}(nm) (10⁻³ ∈ (dm³ mol⁻¹ cm⁻¹)): 362 (54.6), 378 (49.9), 449 (3.90). [Ag(Ph₃P)₂(HaaiEt)]NO₃ (**6a**): Anal. Calcd. for C₄₇H₄₂N₅O₃P₂Ag: C, 55.07; H, 4.62; N, 5.45. Found: C, 54.89; H, 4.68; N, 5.47; FT-IR (KBr disc, cm⁻¹): ν(N=N), 1441; ν(C=N), 1556 cm⁻¹; UV-Vis spectroscopic data in CHCl₃ (λ_{max}(nm) (10⁻³ ∈ (dm³ mol⁻¹ cm⁻¹)): 361 (40.2), 453 (4.4). [Ag(Ph₃P)₂(MeaaiEt)]NO₃ (**6b**): Anal. Calcd. for C₄₈H₄₄N₅O₃P₂Ag: C, 55.73; H, 4.52; N, 5.43. Found: C, 55.62; H, 4.46; N, 5.41; FT-IR (KBr disc, cm⁻¹): ν(N=N), 1440; ν(C=N), 1556 cm⁻¹; UV-Vis spectroscopic data in CHCl₃ (λ_{max}(nm) (10⁻³ ∈ (dm³ mol⁻¹ cm⁻¹)): 363 (47.6), 453 (3.82).

Photometric measurements:

Absorption spectra were taken with a Perkin-Elmer Lambda 25 UV/Vis spectrophotometer in a 1 × 1 cm quartz optical cell maintained at 25°C with a Peltier thermostat. The light source of a Perkin-Elmer LS 55 spectrofluorimeter was used as an excitation light, with a slit width of 10 nm. An optical filter was used to cut off overtones when necessary. The absorption spectra of the *cis* isomers were obtained by extrapolation of the absorption spectra of a *cis*-rich mixture for which the composition is known from ¹H NMR

integration. Quantum yields (φ) were obtained by measuring initial *trans*-to-*cis* isomerization rates (ν) in a well-stirred solution within the above instrument using the equation, ν = (φ I₀/V)(1 - 10^{-Abs}), where I₀ is the photon flux at the front of the cell, V is the volume of the solution, and Abs is the initial absorbance at the irradiation wavelength. The value of I₀ was obtained by using azobenzene (φ = 0.11 for π-π* excitation¹⁹) under the same irradiation conditions.

The thermal *cis*-to-*trans* isomerisation rates were obtained by monitoring absorption changes intermittently for a *cis*-rich solution kept in the dark at constant temperatures (*T*) in the range from 298–313 K. The activation energy (*E*_a) and the frequency factor (*A*) were obtained from the Arrhenius plot, ln *k* = ln *A* - *E*_a/RT, where *k* is the measured rate constant, *R* is the gas constant, and *T* is temperature. The values of activation free energy (Δ*G*^{*}) and activation entropy (Δ*S*^{*}) were obtained through the eq. (1),

$$\Delta G^* = E_a - (RT + T\Delta S^*) \text{ and}$$

$$\Delta S^* = [\ln A - 1 - \ln (k_B T/h)]/R \quad (1)$$

where *k*_B and *h* are Boltzmann's and Plank's constants, respectively.

X-Ray diffraction study:

The block shaped dark colored single crystals of [Cu(PPh₃)₂(HaaiMe)]ClO₄ (**3a**), (0.08 × 0.09 × 0.11 mm³) were grown by slow evaporation of the reaction mixture for a week. An appropriate crystal was mounted on a Siemens CCD diffractometer equipped with graphite monochromated Mo-K_α (λ = 0.71073 Å) radiation. The crystallographic data are shown in Table 6. The unit cell parameters and crystal-orientation matrices were determined by least squares refinements of all the reflections. The intensity data were corrected for Lorentz and polarization effects and an empirical absorption correction were applied. Data were collected applying the condition *I* > 2σ(*I*). The structure was solved by direct method and followed by successive Fourier and difference Fourier

Table 6. Summarized crystallographic data for [Cu(PPh₃)₂(HaaiMe)]ClO₄ (**3a**)

Empirical formula	[Cu(HeaiMe)(PPh ₃) ₂]ClO ₄
Formula weight	C _{45.66} H ₄₀ ClCuN ₄ O ₄ P ₂
Temperature (K)	273(2)
Crystal system	Monoclinic
Space group	P2(1)/n
<i>a</i> (Å)	9.9174(2)
<i>b</i> (Å)	14.7540(3)
<i>c</i> (Å)	29.3832(6)
β (°)	93.4360(10)
<i>V</i> (Å ³)	4291.66(15)
<i>Z</i>	4
μ (Mo-K _α) (mm ⁻¹)	0.71073
θ range	1.39–24.19
<i>hkl</i> range	–11 < <i>h</i> < 11; –17 < <i>k</i> < 16; –33 < <i>l</i> < 33
<i>D</i> _{Calcd.} (mg m ⁻³)	1.332
Refine parameters	542
Total reflections	41790
Unique reflections	6877
R ₁ ^a [<i>I</i> > 2σ (<i>I</i>)]	0.0708
wR ₂ ^b	0.1592
Goodness of fit	1.006
^a R = Σ F _o – F _c / Σ F _o ; ^b wR ₂ = [Σw(F _o ² – F _c ²) ² / Σw(F _o ²) ²] ^{1/2} ; w = 1/[σ ² (F _o) ² + (0.0778P) ² + 9.4074P]; where P = ((F _o ² + 2F _c ²)/3).	

syntheses. Full matrix least squares refinements on *F*² were carried out using SHELXL-97²⁰ with anisotropic displacement parameters for all non-hydrogen atoms. Hydrogen atoms were restricted to ride on the respective carbon or nitrogen atoms with isotropic displacement parameters equal to 1.2 times the equivalent isotropic displacement of their parent atom in all cases. All calculations were carried out using SHELXL 97²⁰, SHELXS 97²¹, PLATON 99²² and ORTEP-3²³ program.

Crystallographic data for the structure of [Cu(PPh₃)₂(HaaiMe)]ClO₄ (**3a**) have been deposited with the Cambridge Crystallographic Data Center, CCDC No. 1580970. Copies of this information may be obtained free of charge from the Director, CCDC,

12 Union Road, Cambridge CB2 1EZ, UK (E-mail: deposit@ccdc.cam.ac.uk or www:htp://www.ccdc.cam.ac.uk).

Computational study:

Gaussian09 program software package²⁴ was used to optimize geometry by DFT computation technique. The basis set B3LYP level^{25,26} were used for C, H, N, O, and the LanL2DZ effective core potential (ECP) set of Hay and Wadt^{27–29} for Cu, Zn and P atoms³⁰. The vibrational frequency calculations were performed to ensure that the optimized geometries represent the local minima and there are only positive eigen values. Vertical electronic excitations based on B3LYP optimized geometries were computed using the time-dependent density functional theory (TDDFT) formalism³¹ in acetonitrile using conductor-like polarizable continuum model (CPCM)³² using the same B3LYP level and basis sets. GAUSSSUM³³ was used to calculate the fractional contributions of various groups to each molecular orbital.

Conclusion

Ag(I)/Cu(I)-triphenylphosphine complexes of 1-alkyl-2-(arylo)imidazoles are described. Upon UV light irradiation to the solution of the complexes the *trans*-geometry changes to *cis*-geometry about -N=N-bond of 1-alkyl-2-(arylo)imidazoles both in free and complexation phase. Quantum yields of *trans*-to-*cis* isomerisation is lower in complex than that of free ligand phase. The *cis*-to-*trans* isomerisation is thermally driven process. The activation energy (*E*_a) of *cis*-to-*trans* isomerisation is lower in complex than that of free ligand which may be the reason for slow transformation.

Acknowledgements

We are thankful to the University Grants Commission for the Research Project (F.PSW-158/13-14) (D. Mallick) and to the Council of Scientific and Industrial Research, New Delhi for the financial support (Sanction No. 01(2894)/17/EMR-II) (C. Sinha).

References

1. M. Cacciarini, A. B. Skov, M. Jevric, A. S. Hansen, J. Elm, H. G. Kjaergaard, K. V. Mikkelsen and M. B. Nielsen, *Chemistry: A Eur. J.*, 2015, **21**, 7454.
2. H. Zollinger, "Diazo Chemistry-I, Aromatic and Heteroaromatic Compounds", Wiley VCH, Germany, 1997.
3. P. Stallnga, "Electrical Characterization of Organic Electronic Materials and Devices", John Wiley & Sons Ltd., 2009.
4. Z. Cui (Ed.), "Printed Electronics: Materials, Technologies and Applications", Chinese Academy of Sciences, China, 2016.
5. C. Winder and N. S. Sariciftci, *J. Mater. Chem.*, 2004, **14**, 1077.
6. J. Otsuki, K. Suwa, K. Narutaki, C. Sinha, I. Yoshikawa and K. Araki, *J. Phys. Chem. (A)*, 2005, **109**, 8064; J. Otsuki, K. Suwa, K. K. Sarker and C. Sinha, *J. Phys. Chem. (A)*, 2007, **111**, 1403.
7. H. Rau, in: "Photochromism, Molecules and Systems", eds. H. Dürr and H. Bounas-Laurent, Elsevier, Amsterdam, 1990, 165; H. Nishihara, *Bull. Chem. Soc. Jpn.*, 2004, **77**, 407; Y. Zhao and T. Ikeda, "Smart Light-Responsive Materials: Azobenzene-Containing Polymers and Liquid Crystals", John Wiley & Sons Ltd., 2009.
8. P. Bhuina, U. S. Ray, G. Mostafa, J. Ribas and C. Sinha, *Inorg. Chim. Acta*, 2006, **359**, 4660; J. Dinda, S. Senapoti, T. Mondal, A. D. Jana, M. Chiang, T.-H. Lu and C. Sinha, *Polyhedron*, 2006, **25**, 1125; T. K. Mondal, J. Dinda, J. Cheng, T.-H. Lu and C. Sinha, *Inorg. Chim. Acta*, 2008, **361**, 2431.
9. N. Fukuda, J. Y. Kim, T. Fukuda, H. Ushijima and K. Tamada, *Jpn. J. Appl. Phys.*, 2006, **45**, 460; G. A. Molander (Ed.), "Science of Synthesis: Houben-Weyl Methods of Molecular Transformations", George Thieme Verlag K.G., Germany, 2007, **33**.
10. S. Saha (Halder), P. Mitra and C. Sinha, *Polyhedron*, 2014, **67**, 321; P. Datta, D. Mallick, T. K. Mondal and C. Sinha, *Polyhedron*, 2014, **71**, 47.
11. K. K. Sarker, D. Sardar, K. Suwa, J. Otsuki and C. Sinha, *Inorg. Chem.*, 2007, **46**, 8291.
12. K. K. Sarker, B. G. Chand, K. Suwa, J. Cheng, T.-H. Lu, J. Otsuki and C. Sinha, *Inorg. Chem.*, 2007, **46**, 670.
13. S. Saha (Halder), S. Roy, T. K. Mondal, R. Saha and C. Sinha, *Z. Anorg. Alleg. Chem.*, 2013, **639**, 1861.
14. P. Pratihar, T. K. Mondal, A. K. Patra and C. Sinha, *Inorg. Chem.*, 2009, **48**, 2760.
15. J. Dinda, S. Senapoti, T. Mondal, A. D. Jana, M. Chiang, T.-H. Lu and C. Sinha, *Polyhedron*, 2006, **25**, 1125; G. Saha, K. K. Sarkar, D. Sardar, J. Cheng, T.-H. Lu and C. Sinha, *Polyhedron*, 2012, **45**, 158.
16. C. Zhang, Y. Song, X. Wang, F. E. Kühn, Y. Wang, Y. Xu and X. Xin, *J. Mater. Chem.*, 2003, **13**, 571.
17. P. Datta, A. K. Patra and C. Sinha, *Polyhedron*, 2009, **28**, 525; P. Gayen and C. Sinha, *J. Luminescence*, 2012, **132**, 2371; P. Gayen, K. K. Sarker and C. Sinha, *Colloids and Surfaces (A)*, 2013, **429**, 60.
18. A. I. Vogel, "A Text-Book of Quantitative Inorganic Analysis", 3rd ed., ELBS, Longman, 1975, 433.
19. G. Zimmerman, L. Chow and U. Paik, *J. Am. Chem. Soc.*, 1958, **80**, 3528.
20. G. M. Sheldrick, SHELXL 97, "Program for the Solution of Crystal Structure", University of Gottingen, Germany, 1997.
21. G. M. Sheldrick, SHELXS 97, "Program for the Solution of Crystal Structure", University of Gottingen, Germany, 1997.
22. A. L. Spek, PLATON, "Molecular Geometry Program", University of Utrecht, The Netherlands, 1999.
23. L. J. Farrugia, "ORTEP-3 for windows", *J. Appl. Cryst.*, 1997, **30**, 565.
24. M. J. Frisch, G. W. Trucks, H. B. Schlegel, G. E. Scuseria, M. A. Robb, J. R. Cheeseman, G. Scalmani, V. Barone, B. Mennucci, G. A. Petersson, H. Nakatsuji, M. Caricato, X. Li, H. P. Hratchian, A. F. Izmaylov, J. Bloino, G. Zheng, J. L. Sonnenberg, M. Hada, M. Ehara, K. Toyota, R. Fukuda, J. Hasegawa, M. Ishida, T. Nakajima, Y. Honda, O. Kitao, H. Nakai, T. Vreven, J. A. Montgomery (Jr.), J. E. Peralta, F. Ogliaro, M. Bearpark, J. J. Heyd, E. Brothers, K. N. Kudin, V. N. Staroverov, R. Kobayashi, J. Normand, K. Raghavachari, A. Rendell, J. C. Burant, S. S. Iyengar, J. Tomasi, M. Cossi, N. Rega, J. M. Millam, M. Klene, J. E. Knox, J. B. Cross, V. Bakken, C. Adamo, J. Jaramillo, R. Gomperts, R. E. Stratmann, O. Yazyev, A. J. Austin, R. Cammi, C. Pomelli, J. W. Ochterski, R. L. Martin, K. Morokuma, V. G. Zakrzewski, G. A. Voth, P. Salvador, J. J. Dannenberg, S. Dapprich, A. D. Daniels, Ö. Farkas, J. B. Foresman, J. V. Ortiz, J. Cioslowski and D. J. Fox, GAUSSIAN 09, Revision D.01, Gaussian Inc., Wallingford, CT, 2009.
25. A. D. Becke, *J. Chem. Phys.*, 1993, **98**, 5648.
26. C. Lee, W. Yang and R. G. Parr, *Phys. Rev. (B)*, 1988, **37**, 785.
27. P. J. Hay and W. R. Wadt, *J. Chem. Phys.*, 1985, **82**, 270.

28. W. R. Wadt and P. J. Hay, *J. Chem. Phys.*, 1985, **82**, 284.
29. P. J. Hay and W. R. Wadt, *J. Chem. Phys.*, 1985, **82**, 299.
30. G. A. Petersson, A. Bennett, T. G. Tensfeldt, M. A. Al-Laham, W. A. Shirley and J. Mantzaris, *J. Chem. Phys.*, 1988, **9**, 2193; G. A. Petersson and M. A. Al-Laham, *J. Chem. Phys.*, 1991, **94**, 6081.
31. R. Bauernschmitt and R. Ahlrichs, *Chem. Phys. Lett.*, 1996, **256**, 454; R. E. Stratmann, G. E. Scuseria and M. J. Frisch, *J. Chem. Phys.*, 1998, **109**, 8218; M. E. Casida, C. Jamorski, K. C. Casida and D. R. Salahub, *J. Chem. Phys.*, 1998, **108**, 4439.
32. V. Barone and M. Cossi, *J. Phys. Chem. (A)*, 1998, **102**, 1995; M. Cossi and V. Barone, *J. Chem. Phys.*, 2001, **115**, 4708; M. Cossi, N. Rega, G. Scalmani and V. Barone, *J. Comput. Chem.*, 2003, **24**, 669.
33. N. M. O'Boyle, A. L. Tenderholt and K. M. Langner, *J. Comput. Chem.*, 2008, **29**, 839.